UCRL-16907

University of California

Ernest O. Lawrence Radiation Laboratory

ANNEALING OF DISLOCATION LOOPS IN ALUMINUM

TWO-WEEK LOAN COPY

This is a Library Circulating Copy which may be borrowed for two weeks. For a personal retention copy, call Tech. Info. Division, Ext. 5545

Berkeley, California

DISCLAIMER

This document was prepared as an account of work sponsored by the United States Government. While this document is believed to contain correct information, neither the United States Government nor any agency thereof, nor the Regents of the University of California, nor any of their employees, makes any warranty, express or implied, or assumes any legal responsibility for the accuracy, completeness, or usefulness of any information, apparatus, product, or process disclosed, or represents that its use would not infringe privately owned rights. Reference herein to any specific commercial product, process, or service by its trade name, trademark, manufacturer, or otherwise, does not necessarily constitute or imply its endorsement, recommendation, or favoring by the United States Government or any agency thereof, or the Regents of the University of California. The views and opinions of authors expressed herein do not necessarily state or reflect those of the United States Government or any agency thereof or the Regents of the University of California.

Special Thesis

UCRL-16907

UNIVERSITY OF CALIFORNIA

Lawrence Radiation Laboratory
Berkeley, California

AEC Contract No. W-7405-eng-48

ANNEALING OF DISLOCATION LOOPS IN ALUMINUM

Jean-Pierre Tartour

(Master's Thesis)

August 1966

ANNEALING OF DISLOCATION LOOPS IN ALUMINUM

Jean-Pierre Tartour

Inorganic Materials Research Division, Lawrence Radiation Laboratory,
Department of Mineral Technology, College of Engineering,
University of California, Berkeley, California

August 1966

ABSTRACT

The change in shape after annealing of Frank loops in quenched 99.999% pure aluminum has been studied by electron microscopy. The loops are found to get roundish at the corners. The process continues until the loops become perfectly round, then they shrink as such upon further annealing. The activation energy for the rounding process is found to be 0.8eV±0.2eV, suggesting that some short circuit diffusion takes place.

A model is tentatively proposed according to which the process should be controlled by the creation of bound vacancies at the pre-existing well-formed jogs.

I. INTRODUCTION

By rapidly quenching a metal from a temperature greater than about two-thirds of its melting point one can retain a large supersaturation of vacancies which will subsequently cluster in various forms. In aluminum the vacancy clusters so fare investigated are:

1. Frank loops; an imperfect dislocation with Burgers vector $\frac{a}{3}[111]$ enclosing a stacking fault. These loops lie in (111) planes, are hexagonal in shape with sides parallel to [110] directions.[1] They are occasionally found to lie in rows or to assume more or less asymmetrical shapes which may be due to the presence of impurities.

2. Glissile prismatic loops; formed either directly or by nucleation of a Shockley dislocation sweeping out the fault of a Frank loop. In the latter case the hexagonal shape is not retained if further growth occurs. By a process of climb and glide,[2] the loop gradually converts to a diamond shape, with sides on (111) planes and a habit plane close to (012).[3,4]

3. Double layer loops of various types first observed by Westmacott et al.[5] An example is shown in Fig. 1.

4. Octahedral voids initially reported by Kiritani,[6] with edges parallel to [110] directions, surrounded by (111) planes.

All of these defects have been observed to shrink upon annealing by emission of vacancies to the nearest sinks or to the surface. The activation energy for the process has been found to be of the order of the self-diffusion energy, i.e., ~1.4eV. Typically, all of these defects get roundish during the early stages of annealing and shrink as such.[7,8,9]

Besides this self-diffusion process a short-circuit diffusion has also been suggested to account for some facts:

1. When annealing in bulk the larger loops have often been observed to grow at the expense of the smaller loops.[16] To explain loop coarsening Johnson has suggested a short-circuit diffusion process, the driving force of which would be the mutual attraction between two close enough loops.[10] By migration of vacancies along the core of the dislocation, combined with some glide, the loops would be able to move towards each other ("conservative climb") and coalesce. However more accurate calculations by Kroupa et al.[11] suggest that the activation energy for the process (if it were actually occurring) would be close to the self diffusion energy. Also the intermediary stages that would be involved in the process are very seldom observed, especially in the case of Frank loops where glide is not possible. The rare examples such as that shown in Fig. 2 can also be explained by considering that two loops have been nucleated in the same atomic layer and have encountered each other during their growth.

Two neighboring loops were sometimes observed to interact with each other upon annealing as shown in Fig. 6. Here a pipe diffusion process may have been involved.

2. Though the loops become roundish upon annealing, some of them keep an angular part which may even grow sharper than it originally was. Shimomura suggests a pipe diffusion process to account for this phenomenon; observing that the polygonal part always faces toward the nearest dislocation line he assumes that its stress field distorts the equilibrium shape of the loop.[9] We also observed a similar behaviour for some loops but were not able to find any correlation between the location of the sharp corner on the loop and the position of the neighboring loops or dislocations as shown in Fig. 3. However, the fraction of loops that

shrank or changed shape irregularly varied from one specimen to another suggesting a pinning of the dislocation by impurities. Because the long single crystals used were grown from the melt there may have been inhomogeneity in the distribution of impurities along the length.

3. Price observed the splitting of long dipoles into rows of loops in zinc.[18] The total area enclosed being conserved, he concluded that the process involved a short-circuit diffusion.

4. Hexagonal loops are sometimes found to get perfectly circular upon annealing.[9] Assuming the circle to be the least energy configuration for these loops the change in shape from hexagonal to circular may occur by conservative climb. For low enough annealing temperature, when bulk diffusion is very much reduced, one might be able to observe the rounding off of the loops to occur without variation of the area enclosed, by diffusion of vacancies along the core of the dislocation. It is the subject of this work to investigate this possibility. Only Frank loops were studied because motion of a $\frac{a}{3}[111]$ dislocation can only take place by climb. Perfect loops can also glide which make observations more difficult.

II. EXPERIMENTAL PROCEDURE

The material used was 99.999% pure aluminum. Strips 1" in width and 20 mils thick were rolled down to a thickness of 8 mils. Six inch lengths were welded onto (112) seeds. The final orientation was adjusted by taking Laue back reflection x-ray pattern, bending the strip with respect to the seed so as to make (112) exactly parallel to the surface. The strip was then tightly packed with graphite powder into a graphite mould and put into a single crystal furnace under high vacuum (the natural gradient of the furnace being used to melt the crystal starting from the top end).

(112) crystals with dislocation density less than 10^6 were thus obtained.

The choice of the (112) orientation is very convenient since it gives one set of loops almost parallel to the surface (angle about 19°), hence projected almost in true shape on the micrograph. The respective position and shape of the four sets of loops are shown in Fig. 1. Another advantage offered by this orientation is that it makes it possible to use a [111] diffracting beam (the closest for a F.C.C. crystal) which gives a very good contrast.

A. Quenching Procedure

Specimens of 1" × 3/4" were cut out of the strips and placed in a holder designed to minimize deformation during quenching. The specimens were held for 30 minutes in a furnace at the bottom of which a slit was cut. A small weight was attached at the bottom of the holder and the quench carried out by dropping into a beaker full of water. The surface of the water was kept as close as possible to the hot zone, i.e., about 1/4 cm. As is well known the kind and size of the defects depend very strongly on the quenching conditions which are difficult to reproduce exactly. There is a rather large dispersion of the results among different investigators and the problem is still being studied. However, some general tendencies can be outlined:[6]

1. The loops are all faulted except when the internal stresses resulting from the quench are too high and remove the fault.
2. The size of the loops decreases when the quenching temperature is increased, everything being kept constant otherwise.
3. The size of the loops decreases when the temperature of the quenching bath is decreased.

For these experiments the specimens were quenched from 605°C into

water at 85°C. The loops obtained were 3000 Å in diameter or larger and their density rather low ($\sim 5.10^{11}/cm^3$), thus avoiding unwanted interactions between loops. An aging temperature of 95°C gave loops that were too large (up to 9000 Å) and therefore easily converted to perfect loops during handling or by the stresses that developed during observation in the electron microscope. On the other hand, for an aging temperature of 70°C the loops were only 1000-1500 Å in diameter. After quenching the specimens were kept for a few days at room temperature.

B. Preparation of the Thin Foils

The specimens were electropolished in a 80% methyl alcohol-20% perchloric acid (70%) solution at -20°C. A stainless steel beaker was used as the cathode. The specimen was suspended from a clamp into the bath. The polishing was carried out at 17V and $0.07 A/cm^2$. The usual window technique was used, the specimen being turned upside down as soon as a hole appeared at the top part. After 2 or 3 such operations a uniformly thin specimen was obtained. The voltage was then lowered down to 10V in order to avoid damaging the edges of the foils and the power was switched on and off. Small pieces were thus detached which could be collected as they fell away from the edges of the specimen. The procedure minimized the chances of accidental bending of the foils. The thin foild were then repeatedly washed in 200 proof ethyl alcohol and kept in it until observation.

C. Microscopy

The observations were carried out using a Siemens Elmiskop I electron microscope operated at 100 KV. The specimens were mounted between two 75 mesh grids. The use of a single tilting stage, though not too convenient, was imposed by the annealing procedure described below. A

manual rotation of the grids was sometimes necessary to achieve the desired orientation. All pictures were taken using the [111] diffracting beam in an orientation always less than a few degrees off the exact (112). A large positive s was used in order to avoid the fringes due to the stacking-fault. Strong fringes make it difficult to determine the actual shape of the loop as shown in Fig. 4, where the sides of the loops appear not to be straight. Whenever possible, that is when the loop was not too close to the surface or the region not too thin, diffraction conditions were adjusted to give a uniform dark shadow enclosed by a dark line. This was assumed to represent the actual shape of the loop. Even if this is not exactly true it can at least be assumed that for equivalent diffraction conditions changes in the shapes of the images represent corresponding changes in the shapes of the loops. Pictures were taken in rather thick regions (about 6000 Å to 8000 Å) for the reason stated above and also to minimize to some extent the chances of nucleation of a Shockley dislocation thereby removing the fault according to the reaction:

$$1/3[111] + 1/6[11\bar{2}] \rightarrow 1/2[110]$$

Despite the care taken to avoid it, this reaction did occur very often. This was a major difficulty in carrying out the experiments. As is well-known, loops of the size observed are unstable at room temperature but because of the high energy of activation necessary to nucleate the Shockley partial they can remain in an unstable equilibrium.[17] Actually, especially for large loops (> 4000 Å), the nucleation occurred rather frequently and even with a beam current kept at its minimum, i.e., 2 to 3 μA and an observation time no longer than two minutes, the thermal stresses induced were often enough to remove the fault.

D. Annealing

A set of twelve pictures was taken before annealing. A map of the specimen was drawn and the various areas photographed were plotted as carefully as possible on it (characteristic pieces of surface dirt were found very useful in locating an area). The specimen holder was then removed from the microscope and its cap unscrewed from the body leaving the specimen sandwiched between the two grids with the cooling ring holding them together. It was assumed that the specimen was not significantly heated during observation (low beam current and total observation time less than 30 minutes). The cap was then introduced into a tube furnace with an atmosphere of argon. The temperature of the furnace was controlled within ±1°C and the rise and fall in temperature at the beginning and at the end of the heating cycle were recorded. The annealing time was slightly corrected to take these transitory periods into account. Heating cycles were carried out at temperatures ranging from 80°C to 130°C and for periods of time from 10 minutes to several hours. Several successive observations were attempted on the same specimen but without much success so far. It was generally impossible to observe the same loops after several anneals because of: specimen getting jammed between the grids, impossibility to get the same orientation, hence the [111] beam, area lost, loops disappearing. Therefore the results given below correspond to single anneals.

E. Measurements

The measured parameter defining the shape of the loops after annealing was the radius of curvature at both ends of the larger diagonal of the loop (parallel to the plane of the micrograph for an exact (112) orientation). As already stated the foils were generally less than 4 or 5° off

the exact orientation so that no significant correction had to be made. The micrographs were taken at a constant magnification of 20,000 then blown up to 70,000 during printing. The measurements were carried out by directly matching on the photographs, circles of various radii with the roundish corners of the loops.

III. EXPERIMENTAL RESULTS

A first way to show the occurrence of pipe-diffusion would be to compare the areas of the loops before and after annealing or rather the lengths a and a' (Fig. 16). If only pipe-duffusion occurs we should have $a' > a$ and $d < c$. However, although we can clearly see in Figs. 5 and 6 that d is smaller than c, the comparison between a and a' is rather subjective for the following reasons: because of the large value of s used (imposed by the presence of fringes) the contrast is often poor. The images of the loops are surrounded by a region of light shadow too strongly dependent on the value of s to be perfectly controlled while taking the micrographs; it may also be affected by the probable alteration of the foil surface upon annealing and, in any case, the possible increase of a would not be very large, since for a circle and a hexagon of same area (Fig. 16), $a = \sqrt{\frac{\pi\sqrt{3}}{6}}\, b = 0.952\ b$ or $\frac{b-a}{b} = 5\%$. However, a close observation of these pictures leaves little doubt that a does not increase but remains approximately constant. Therefore, if some pipe-diffusion is involved its direct effect on the shape of the loop is completely masked by the occurrence of bulk diffusion. Figures 7 and 8 show some loops before annealing and after they have become completely circular. Even at this stage b is at least as large as a confirming the hypothesis that the loops become round before they start shrinking.

Consequently another method was used which allowed us to make an estimate of the activation energy for the rounding process. Various annealing treatments were carried out on different specimens and Figs. 12, 13, 14 and 15 show some typical areas corresponding to each of these annealing stages. For each annealing the radius of curvature R was measured at both ends of the [110] direction parallel to the micrograph for a large number of loops (about 30 to 40) and an average was taken. An example of the distributions obtained is shown in Fig. 17. It correspond to the loops of Figs. 10 and 11. The dispersion is rather wide and sometimes different radii were measured at different corners of the same loop. No correlation could be made between the rate of rounding and the position of the loop with respect to the surface (as determined from the aspect of the fringes). However a general tendency toward slightly larger radii for smaller loops was observed. The apparent activation energy was determined assuming a law of the form $R = f[t \exp(\frac{E}{kT})]$ (the observations suggest that f should be linear, Fig. 9). At 130°C an annealing time of 20 minutes was enough to cause average sized loops to become completely round. No experiments were carried out at higher temperature, because the process occurred too fast to be measured. The lowest temperature used was 80°C and the annealing time about 20 hours. The results were plotted on a semi-logarithmic scale (Fig. 18). Each point represents one annealing. The corresponding measurements of the radii of curvature are reported in Table 1. The straight lines join equivalent states of annealing as defined by the particular radius of curvature at the corners. The three lines correspond to radii of 460Å, 570Å and 900Å respectively. The activation energy was found to be 0.8eV. This is much lower than the energy for self-diffusion in aluminum, which is 1.4eV.

The error on the value of E is of the order of 0.2eV. It comes mainly from the uncertainties on the temperature known only to ±1°C and on the time, especially for the shorter annealings.

IV. DISCUSSION

It is clear from the observations that the loops become round before they start to shrink appreciably. Although no direct evidence of conservative climb could be observed (a was always found to be equal to a' within the accuracy of the measurements), the value of the activation energy for the process was found to be much lower than that for self-diffusion which suggests that the rounding off of the corners of the loops might involve a process more energetically favorable than that proposed by Silcox and Whelan[7] for the shrinkage. These authors assumed that vacancies are emitted at the jogs and that the circular shape is retained by a "coincidental" equilibrium between the rate of formation of the jogs at the corners of the loop and their velocity along the straight sides. A more promising explanation appears to be to assume that elastic strain energy is minimized by a circular shape and that when the loops are not growing they tend to assume this shape by diffusion of vacancies along the dislocation core combined with self-diffusion. No attempt has been made so far to compare the elastic strain energy of hexagonal and circular loops of the same area taking into account the anisotropy of the crystal and the core energy. Using Kroner's calculation method,[20] Hirth et al.[13] predict comparable energies, within a small fraction of the core energy, for the hexagon and the circle. The method consists essentially in setting the self-elastic energy of the loop equal to one half of the interaction energy between two identical loops with opposite Burgers vectors very close to each other, for instance lying in two parallel

planes a distance t apart from each other. Taking t equal to twice the dislocation width, the authors suggest that the core energy should thus be included in their results. A more reliable calculation seems to be that of Bacon et al.[12] who use the same method but set t equal to the core radius. Their justification for this choice is that it gives the same results as Yoffe's method (the usual volume integral for the energy is transformed into a surface integral on a cut ending on the dislocation line).[21] To this first term they add a second one corresponding to the integration on the surface of the core. Setting the core radius equal to $\frac{5}{3}b$ where b = 2.86Å in aluminum, their results for the perfect edge orientation are as follows: for a radius R of the circle equal to 1100Å the energy of the hexagon and the circle are 9287 and 9038 respectively (in arbitrary units); for R = 550Å they become 4128 and 4027. Hence a relative variation of about 2.5%. Because of the small magnitude of this variation on one hand, and of the probable effect of the core energy, the anisotropy of the crystal and the presence of a stacking-fault on the other hand, these results should only be considered as a hint which confirms our previous assumption that the circle is the minimum energy configuration. It may be worth noting here that the intuitive idea that the round shape corresponds to the least length of dislocation for a given area of the loop is no longer true when the periodicity of the lattice is taken into account and the circle resolved in terms of jogs. Actually, the circle <u>inscribed</u> in the hexagon has the same length as the hexagon itself, as can be checked easily by adding up all the segments of dislocation. However, for a jog, only the core energy has to be taken into account since at long range its effect is rapidly blurred by the stress-field of the whole dislocation.

A possible explanation of the observed hexagonal Frank loops would be that the dislocation which surrounds the fault takes a position of least energy along the [110] close-packed directions in the (111) planes. This is equivalent to assuming a very high jog energy. This very crude approximation should not hold if our assumption is to be true. Alternatively the hexagonal shape may be merely the result of the process of growth of the loops. Saada[14] made a calculation of the equilibrium shape of a loop in the presence of a supersaturation of vacancies, taking into account the anisotropy of the crystal. He found that the lower the temperature at which the loops grow the sharper should be the corners of the polygon; hence the hexagonal shape for loops formed by quenching. Thomson et al.[15] have suggested that during loop growth the jogs pre-existing on the sides will spread by absorption of vacancies, until they annihilate by collision with one another or go to a corner where they are slowed down in their motion by the already tightly packed jogs there. The jogs being preferential sites for condensation of vacancies, their velocity should be high enough for the process not to be overwhelmed by the nucleation of new jogs. On the other hand the strong repulsion from the corners should prevent any nucleation there. Hence the loops should end up with straight sides.

A last argument against a "coincidental" round shape resulting from some equilibrium between the rate of emission of vacancies at the corners of the loops and the velocity of the jogs thus formed might be that for fast enough shrinking irregular shapes are often observed which suggests that the circle is a configuration of <u>static</u> equilibrium.

In the next paragraph a model for the process is proposed.

V. MODEL FOR THE PROCESS

Many difficulties arise when trying to build a model for the process. First there is no available calculation for the elastic strain energy of a loop in an anisotropic medium, hence for the climb force which tends to make the loop circular. On the other hand this force is not uniform along a straight side, but must be maximum at a corner and vanish at the middle of the side by symmetry (we are only considering here the component of the force parallel to the side). This force must also vary as the shape of the loop changes, decreasing as the equilibrium shape is approached; hence a study of the kinetics of motion of the vacancies along the dislocation seems to be prohibitively complicated.

We will therefore restrict our study to a qualitative one, using a very simple model with the following assumptions:

1. Shape of the loop: perfectly circular corners connected by straight segments of dislocation, Fig. 19. (Strongly suggested by the observations.)

2. The process occurs by production of "bound vacancies" (or jog pairs) on the dislocation core in the plane of the loop. These jog pairs will be formed most easily at the corners or at the preexisting well isolated jogs separated by more than four atomic diameters from another jog of opposite sense.

a. At a jog: the creation of a bound vacancy necessitates the formation of two extra jogs (at least as far as the dislocation length is concerned); Fig. 20a.

b. On a straight segment: four jogs are required to create a bound vacancy. Tow configurations are possible, one of which (Fig. 20c) might contribute to the process of rounding of loop corners. For the other configuration (Fig. 20b) the driving force for the process tends to

destroy the jog pair as soon as it is created. In Fig. 20c the interstitial moving towards the corner will either annihilate on a vacancy coming from the corner or else reach the corner (or the first jog on its path), contributing in the second case to the rounding process. In the first case there is no contribution. The relative probability of forming a bound vacancy at a given jog and on straight segment is then of the order of $p = \exp\frac{(2U_j)}{kT}$. Taking $T = 360°K$ and $U_j = 0.1eV$ (Friedel),[19] we get: $p = 525$. Even for the larger loops (5000Å in diameter) the number of sites on a side is less than 1000; on the other hand only one half of the jog pairs created on a straight segment contribute to the process; their effect on the final shape of the loop should therefore be rather small (especially as the number of jogs increases) and we will neglect it in the following development.

Once a jog pair is created the bound vacancy thus formed will move towards the middle of the side (under the action of the force which tends to make the loop circular) until it reaches the next jog or jumps into the lattice.

3. All jogs are of height a (interatomic distance), and the vacancies do not catch one another when moving along the sides, i.e., no relatively stable divacancies or higher order aggregates, which would slow down the process, are formed.

A. Annealing in Thin Foils: Rounding Process

We assume the process to be emission controlled, i.e., we take the vacancy concentration at its equilibrium value everywhere in the lattice. Let $J(x,t)$ and $V(x,t)$ be respectively the probabilities of having a jog or a vacancy at the site defined by x, at time t. Let $F(x,t)$ be the force

due to the line tension and $F_t(x,t)$ and F_n its components parallel and normal to the dislocation line respectively (more precisely $\frac{a\partial F_t(x,t)}{\partial x}$ is the force which favours the movement of the vacancies along the dislocation whereas F_n is approximately constant and equal to the usual force due to the line tension in a circular loop).

The detailed balance of the exchanges with the lattice and along the dislocation gives for the equation of motion of the jogs:

$$\frac{\partial J}{\partial t} = -J(x)\nu_D(x) + J(x+a)\nu_D(x+a) - J(x)\nu_L(x+a) + J(x-a)\nu_L(x)$$

$$+J(x-a)V(x+a)\nu_{vj}(x+a) - J(x)V(x+2a)\nu_{vj}(x+2a) - J(x)\nu_{jv}(x)$$

$$+J(x+a)\nu_{jv}(x+a) + J(x+a)\overrightarrow{\nu_P}(x+a) - J(x)\overrightarrow{\nu_P}(x)$$

$$-J(x)V(x)\overleftarrow{\nu_P}(x) + J(x-a)V(x-a)\overleftarrow{\nu_P}(x-a)$$

where the various terms in the right hand side are respectively: the variations per unit time of the probability of having a jog at x, owing to:

1. Emission at a jog of a vacancy into the lattice (Fig. 21a).

$\nu_D = z\nu\exp(-[U_D - aF_t - \frac{a\sqrt{3}}{2}F_n - \gamma a^2\frac{\sqrt{3}}{2}]/kT)$, where ν is the basic lattice frequency, z is the number of lattice sites around an atomic position in the dislocation, U_D is the activation energy for self-diffusion, γ is the stacking-fault energy, and a the interatomic distance.

2. Jump of a vacancy from the lattice onto a jog (Fig. 21b).

$\nu_L = z\nu\exp(-[U_D + aF_t + a\frac{\sqrt{3}}{2}F_n + \gamma a^2\frac{\sqrt{3}}{2}]/kT)$.

3. Jump of a vacnacy along the dislocation line onto a jog (Fig. 21c).

$\nu_{vj} = \nu\exp(-[U_{pd} - 2U_j - a^2\frac{\partial F_t}{\partial x} + \gamma a^2\frac{\sqrt{3}}{2}]/kT)$. U_{pd} is the energy for pipe-diffusion. We take $2U_j$ for the binding energy between a vacancy and a well-formed jog (on the dislocation line). $a^2\frac{\partial F_t}{\partial x}$ is the work of F_t

during the displacement of the two jogs of opposite sense corresponding to the vacancy. We add $\gamma a^2 \frac{\sqrt{3}}{2}$ to the energy of jump considering that the area of stacking-fault associated with a single vacancy on the dislocation is most certainly less than $a^2 \frac{\sqrt{3}}{2}$ and probably negligible.

4. Emission of a vacancy on the dislocation from a jog (Fig. 21d).

$\nu_{jv} = \nu\exp(-[U_{pd} + 2U_j + a^2 \frac{\partial F_t}{\partial x} - \gamma a^2 \frac{\sqrt{3}}{2}]/kT)$.

5. Formation of a bound vacancy at a jog (Fig. 21c).

$\nu_P^{\rightarrow} = \nu\exp(-[\alpha U_{pd} + 2U_j - aF_t - a^2 \frac{\partial F_t}{\partial x} - \gamma a^2 \frac{\sqrt{3}}{2}]kT)$. α is a coefficient between 1 and 2 which takes into account the fact that the vacancy has to make more than one single jump in order for a jog pair to be formed. The presence of the stacking fault energy term can be explained as in (3).

6. Destruction of a jog pair at a jog (Fig. 21f).

$\nu_P^{\leftarrow} = \nu\exp(-[\alpha U_{pd} - 2U_j + aF_t + a^2 \frac{\partial F_t}{\partial x} + \gamma a^2 \frac{\sqrt{3}}{2}]/kT)$.

Similarly we get for the equation of motion of the vacancies:

$$\frac{\partial V}{\partial t} = [1-J(x-a)]\nu_L'(x) - V(x)\nu_D' - V(x)\nu_{pd}^{\rightarrow}(x)[1-J(x-2a)] + \nu_{pd}^{\rightarrow}(x+a)V(x+a) \ldots$$

$$\ldots [1-J(x-a)] - V(x)\nu_{pd}^{\leftarrow}(x)[1-J(x)] + V(x-a)\nu_{pd}^{\leftarrow}(x-a)[1-J(x-a)]$$

$$+ J(x-a)\nu_{jv}(x-a) - V(x)\nu_{vj}(x)J(x-2a) + J(x+a)\nu_P^{\rightarrow}(x+a) - V(x)J(x)\nu_P^{\leftarrow}(x)$$

where:

7. ν_L' is the jump frequency of a vacancy from the lattice onto the dislocation. $\nu_L' = z\nu\exp(-[U_D + 2U_j + aF_n \frac{\sqrt{3}}{2}]/kT)$.

8. ν_D' is the jump frequency of a vacancy from the dislocation into the lattice. $\nu_D' = z\nu\exp(-[U_D - 2U_j - aF_n \frac{\sqrt{3}}{2}]/kT)$.

9. $\nu_{pd}^{\rightarrow}$ is the jump frequency of a vacancy on the dislocation and to the right (Fig. 19). $\nu_{pd}^{\rightarrow} = \nu\exp(-[U_{pd} - a^2 \frac{\partial F_t}{\partial x}]/kT)$.

10. $\nu_{pd}^{\leftarrow}$ is the jump frequency of a vacancy along the dislocation and to the left. $\nu_{pd}^{\leftarrow} = \nu\exp(-[U_{pd} + a^2 \frac{\partial F_t}{\partial x}]/kT)$.

In these equations we do not take into account some reactions corresponding to the highly improbable configurations shown on Fig. 22. On the other hand the model breaks down at the corners where the jog concentration becomes close to 1 and reactions involving jogs of height larger than one interatomic distance become preponderant. In any case even under this form a complete solution of the problem seems impracticable. Our only purpose in writing down these equations was to determine what reactions might be involved in the process and the corresponding activation energies.

Taking $\gamma = 250$ ergs/cm^2 and $a = 2.86$Å we get: $\gamma a^2 \frac{\sqrt{3}}{2} = 0.11$eV. There is no experimental value for U_{pd}. However, it is generally assumed to be of the order of the migration energy of a vacancy and probably a little less. We will take $U_{pd} = 0.5$eV. $U_D = 1.48$eV[22] and $U_j \sim 0.1$eV. In order to make an estimate of F_t we can assume that this force is due to the action of two segments of dislocation of length $2L\sqrt{3}$, parallel to Oy and located at $x = L$ and $x = -L$ respectively (where 2L is the length of a side of the hexagon). We get:

$$F_t = \frac{\mu b^2 La\sqrt{3}}{8r(1-\nu)}\left(\frac{1}{(L-x)^2} + \frac{1}{(L+x)^2}\right), \text{ hence } aF_t = 0.28\left(\frac{La}{(L-x)^2} + \frac{La}{(L+x)^2}\right)\text{eV}$$

Therefore except for the jogs very close to the corners aF_t should be small probably less than 0.1eV. (Actually the interactions due to the other jogs smooth the variations of F_t with respect to x, decreasing the above value at the corners and increasing it away from the corners.)

From these considerations we may assume that the process of rounding occurs in the following way: bound vacancies are formed at the pre-existing jogs. The vacancy thus "freed" moves away from the jog under the action of the force which tends to make the loop circular and either

jumps into the lattice or reaches the first jog on its path. Thus the reaction limiting the process would be the production of a jog pair. With the values we chose for the various energies involved the activation energy for this reaction would be of the order of that found experimentally for the rounding process, i.e., 0.8eV.

B. Shrinkage of the Loops

When the loop is completely round the force acting on the vacancies on the dislocation line must vanish, therefore once a jog pair is formed the jog is "saturated" by the vacancy thus "freed" and the vacancy must jump into the lattice before a new pair can be formed, or equivalently the pair is destroyed by the inverse reaction and the activation energy for shrinkage is of the order of that for emission at a jog, i.e., $\sim U_D$.

In the case of annealing in the bulk and for a high enough loop concentration, Shimomura[9] finds that the Frank loops retain a somewhat polygonal form while shrinking which may be tentatively explained in the following way: owing to the large number of shrinking loops the vacancy concentration can no longer be assumed to have its equilibrium value (corresponding to the given annealing temperature) but must be much higher and the jump of vacancies from the lattice onto the dislocation becomes important. Therefore along with the shrinkage a process equivalent to growth occurs leading to a final shape which is intermediary between the circle and the hexagon.

VI. CONCLUSIONS

When annealed in thin foils and for low enough rates of shrinkage all Frank loops become perfectly round (except for some pinning by impurities) before shrinking then shrink as such. This rounding process can be observed at much lower temperatures than the shrinkage itself.

Though no clear evidence of conservative climb could be directly obtained, a measurement of the activation energy for the process gave a value of 0.8eV, which strongly suggests that pipe-diffusion was involved. No influence of the proximity of surface could be detected, as expected if emission rather than diffusion controls annealing in thin foils. However, slightly faster rates of rounding for smaller loops were observed. According to our model the process should be controlled by the production of bound vacancies at the jogs.

ACKNOWLEDGEMENTS

The author expresses his gratitude to Professor Jack Washburn for his continued interest and encouragement and to Professor Gareth Thomas for helpful suggestions. This work was supported under the auspices of the United States Atomic Energy Commission through the Inorganic Materials Research Division at the Lawrence Radiation Laboratory, Berkeley.

REFERENCES

1. D. Kuhlman Wilsdorf, Phi. Mag. 3, 125 (1958).
2. G. Thomas and J. Washburn, Rev. of Mod. Phys. 35, 992 (1963).
3. M. J. Makin and B. Hudson, Phil. Mag. 8, 447 (1963).
4. R. Bullough and A. J. E. Foreman, Phil. Mag. 9, 315 (1964).
5. K. H. Westmacott, R. S. Barnes, D. Hull and R. E. Smallman, Phil. Mag. 6, 929 (1961).
6. M. Kiritani, J. Phys. Soc.(Japan) 19, 618 (1964).
7. J. Silcox and M. J. Whelan, Phil. Mag. 5, 1 (1960).
8. J. W. Eddignton and R. E. Smallman, Phil. Mag. 11, 1109 (1965).
9. Y. Shimomura, J. Phys. Soc. (Japan) 20, 965 (1965).
10. C. A. Johnson, Phil. Mag. 5, 1255 (1960).
11. F. Kroupa, J. Silcox and M. J. Whelan, Phil. Mag. 6, 971 (1961).
12. D. J. Bacon and A. G. Crocker, Phil. Mag. 11, 195 (1965).
13. J. P. Hirth, T. Jøssang and J. Lothe, J. Appl. Phys. 37, 110 (1966).
14. G. Saada, Acta Met. 7, 367 (1959).
15. R. M. Thomson and R. W. Balluffi, J. Appl. Phys. 33, 803 (1962).
16. R. Vandervoort and J. Washburn, Phil. Mag. 5, 24 (1960).
17. G. Saada, J. Phys. Soc. (Japan) 18 (III), 41 (1963).
18. P. B. Price, Electron Microscopy and Strength of Crystals (John Wiley and Sons, New York, 1963).
19. J. Friedel, Dislocations (Pergamon Press, New York, 1964).
20. E. Kröner, Kontinuumstheorie der Versetzungen und Eigenspannungen (Springer-Verlag, Berlin, 1958).
21. E. H. Yoffe, Phil. Mag. 5, 161 (1960).
22. S. Kabemoto, J. Appl. Phys. (Japan) 4, 896 (1965).

TABLE I

Temperature (°C)	Annealing Time (min)	Radius of Curvature (Å)
83	126	320
83	190	460
83	284	570
96	151	>970
101	76	820
101	116	970
101	135	1100
102	62	820
103	91	970
103	111	1000
112	46	570
113	20	460
126	15	820
127.5	25	1200
129	20	>820
131	10	460

FIGURE CAPTIONS

Fig. 1 Typical (112) orientation showing the four sets of loops (one of which is seen edge-on = B). Double faulted loops at A.

Fig. 2 Two loops (maybe three) growing on the same atomic plane coalesce to give an elongated loop. (Annealing: 62min at 102°C).

Fig. 3 After annealing at 127.5°C for 25 min some loops conserve an angular part. The location of the sharp corner is completely at rondom suggesting some pinning by impurities. (Marking = 0.5μ).

Fig. 4 Strong fringe contrast. s = 0 in (a) and s slightly negative in (b). (Marking = 0.5μ).

Fig. 5 Same area before and after annealing at 102°C for 62 min. The corners get roundish without any clear change on the straight sides. The dimension of the loop along $\vec{g}$ is practically unchanged or may be somewhat larger in (b).

Fig. 6 Same area before and after annealing at 101°C for 116 min. Same remarks as in Fig. 5. On the other hand, the two neighboring corners have clearly moved toward each other and the two neighboring parallel sides are more inclined on the horizontal in (b) than in (a) suggesting the occurrence of pipe-diffusion along these sides due to the interaction between the two loops.

Fig. 7 Same area for various annealing times at 80.10°C. (0 min., 316 min., 717 min., 1079 min., and 1417 min., respectively).

Fig. 8 Same as Fig. 7.

Fig. 9 Radius of curvature vs time for the loops of Figs. 7 and 8.

Fig. 10 Various areas of the same specimen for an annealing at 102°C for 62 min., showing the dispersion of the radii of curvature. Note the larger radii for the smaller loops. (continued on Fig. 11). (Marking = 0.5μ).

Fig. 11 See Fig. 10.

Fig. 12 a) 76 min at 101°C.

b) 116 min at 101°C.

Fig. 13 a) 46 min at 112°C.

b) 91 min at 103°C.

c) 20 min at 113°C.

d) 190 min at 83°C.

Fig. 14 a) 135 min at 101°C.

b) 111 min at 103°C.

c) 10 min at 131°C.

d) 151 min at 96°C.

Fig. 15 a) 20 min at 129°C.

b) 15 min at 126°C.

c) 126 min at 83°C.

d) 284 min at 83°C.

Fig. 16 Transition from the perfect hexagon to the circle. The broken line corresponds to the [110] direction parallel to the micrograph.

Fig. 17 Distribution of the measurements for the loops of Figs. 10 and 11.

Fig. 18 Plot of annealing time vs temperature. The straight lines join equivalent states of annealing as defined by the particular radius of curvature at the corners. (1) corresponds to an average radius of curvature of 460Å, (2) to 570Å and (3) to 900Å.

Fig. 19 Schematic shape of a roundish loop.

Fig. 20 a) Nucleation of a jog pair at a corner.

b) Nucleation on a straight side. Here the pair should be destroyed right after its formation.

c) Alternative way of creating a pair on a straight side.

Fig. 21 Reactions taken into account in the calculation.

Fig. 22 Reactions neglected in the calculation.

a) Saturation of a jog by a pair.

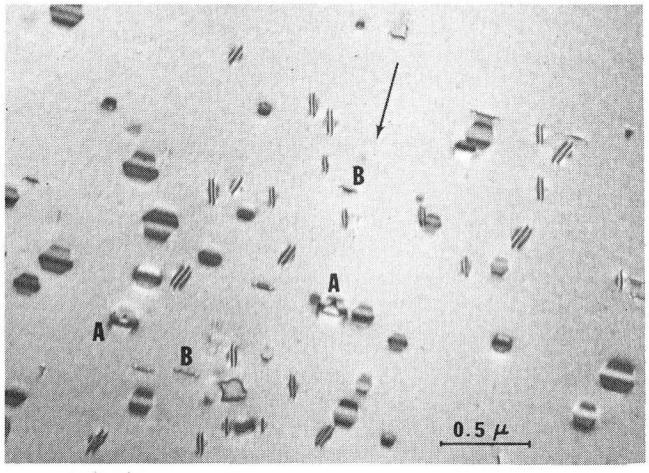

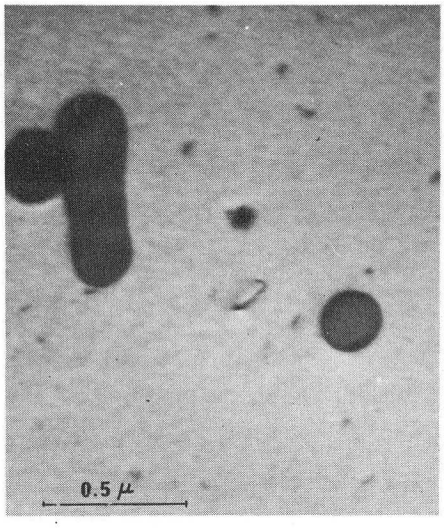

ZN-5878

Figs. 1 and 2

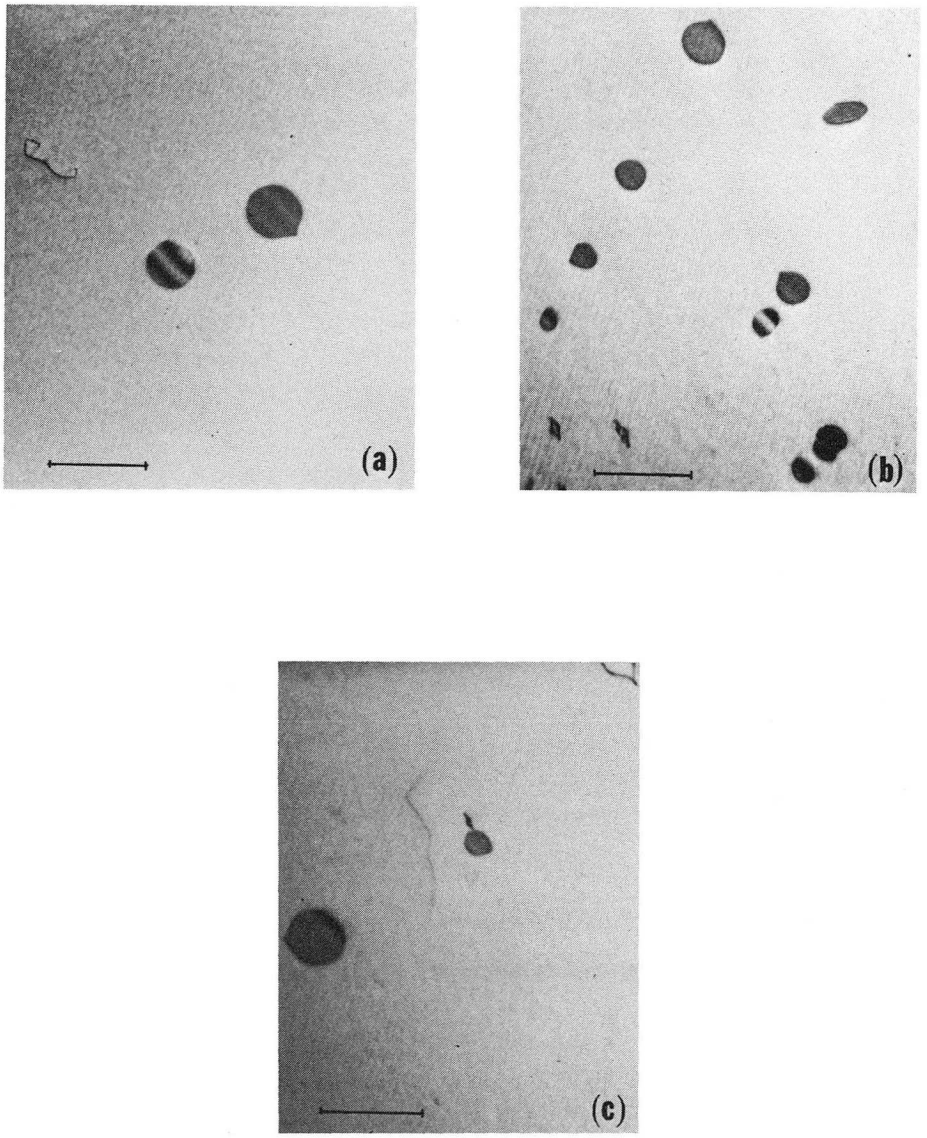

ZN-5871

Fig. 3abc

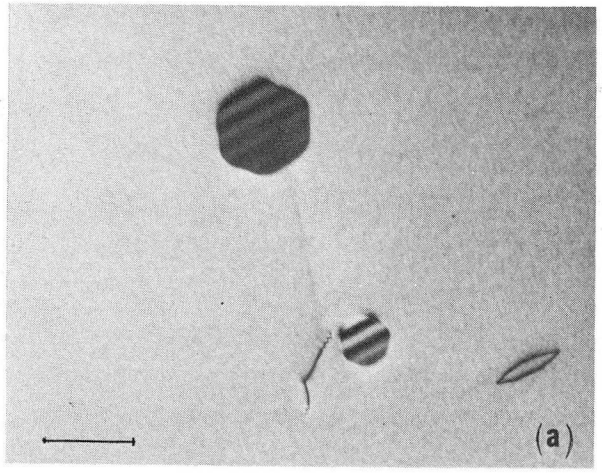

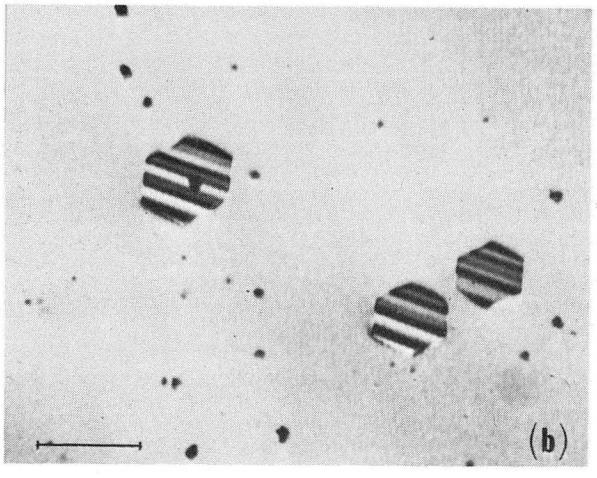

ZN-5877

Fig. 4ab

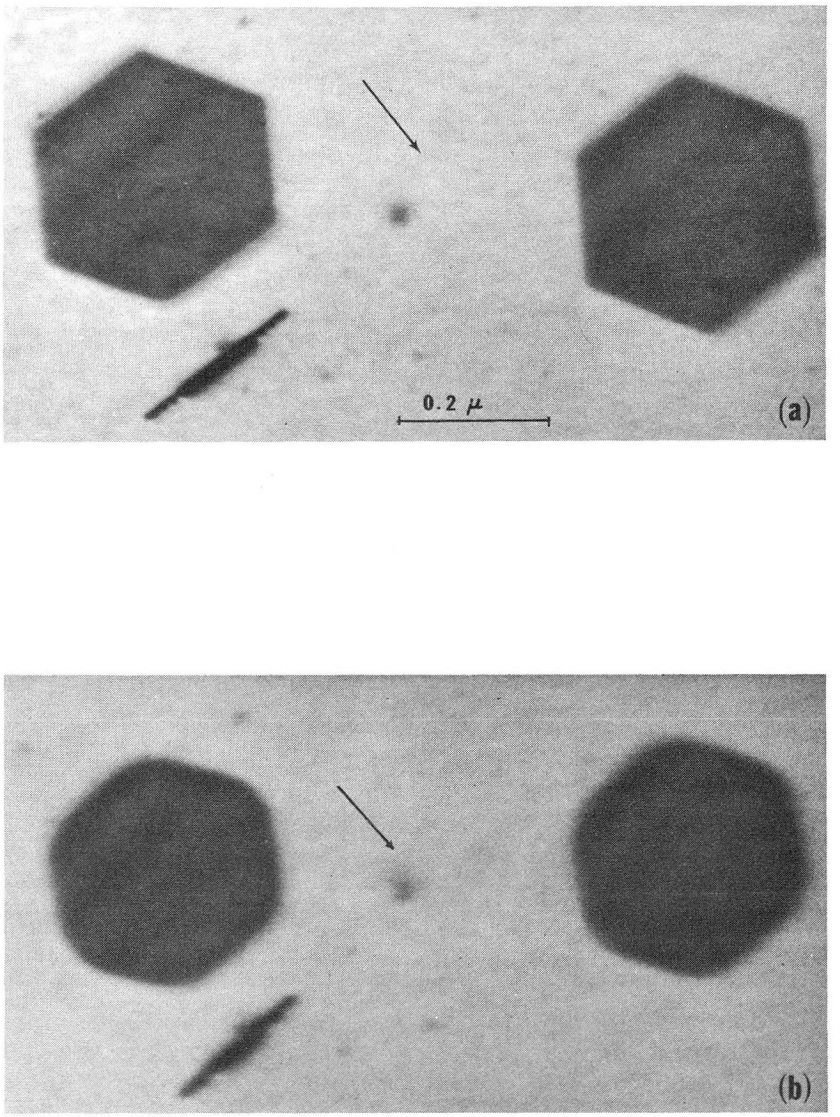

ZN-5881

Fig. 5ab

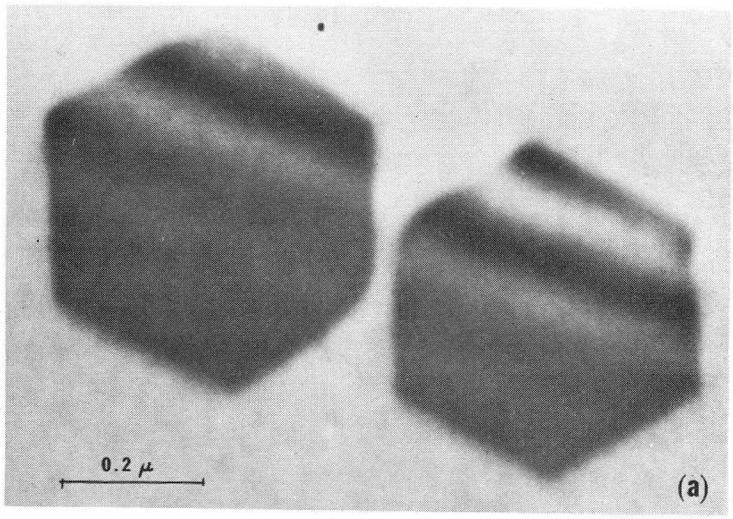

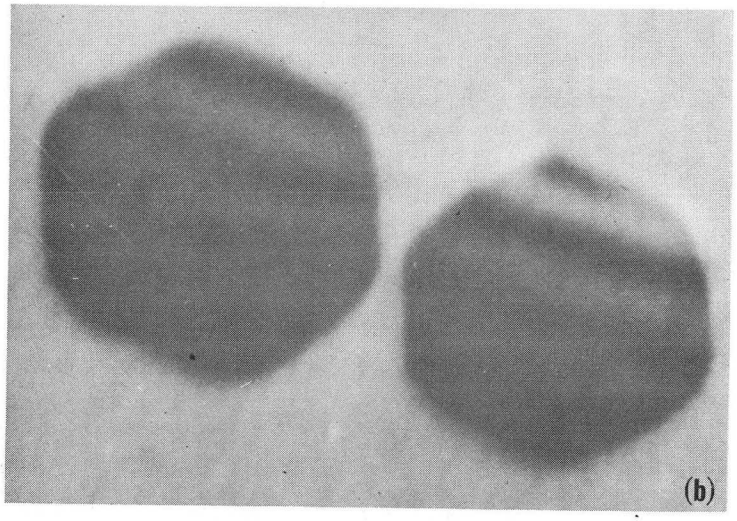

ZN-5875

Fig. 6 ab

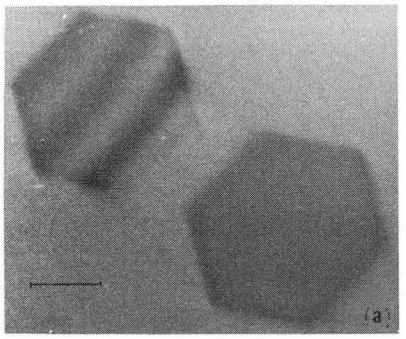

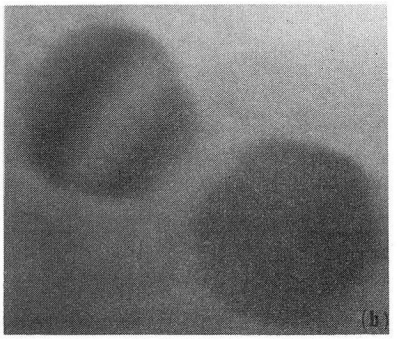

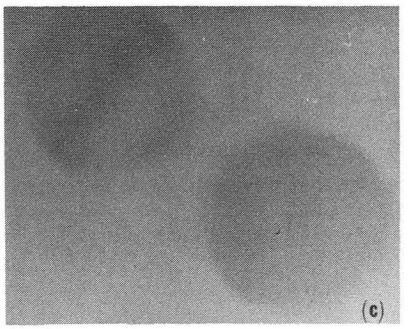

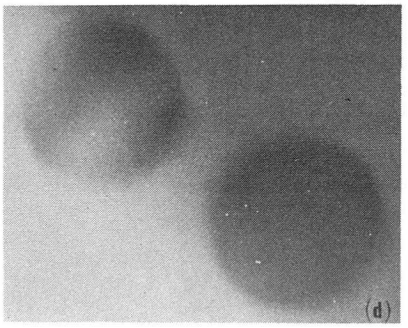

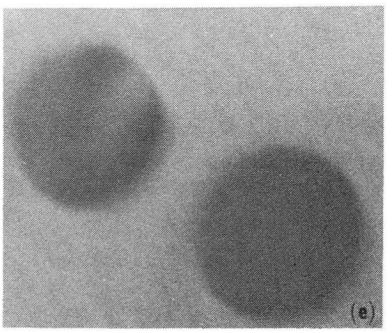

ZN-5872

Fig. 7 abcde

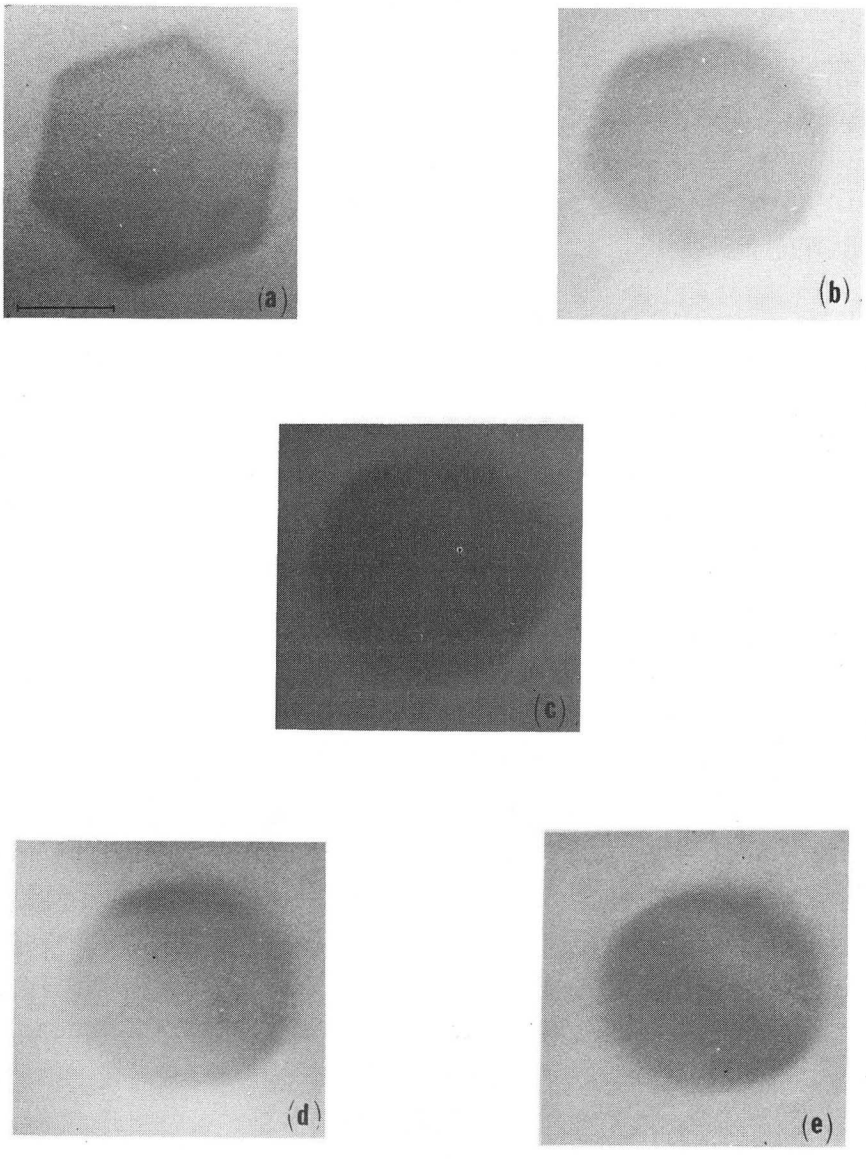

ZN-5873

Fig. 8abcde

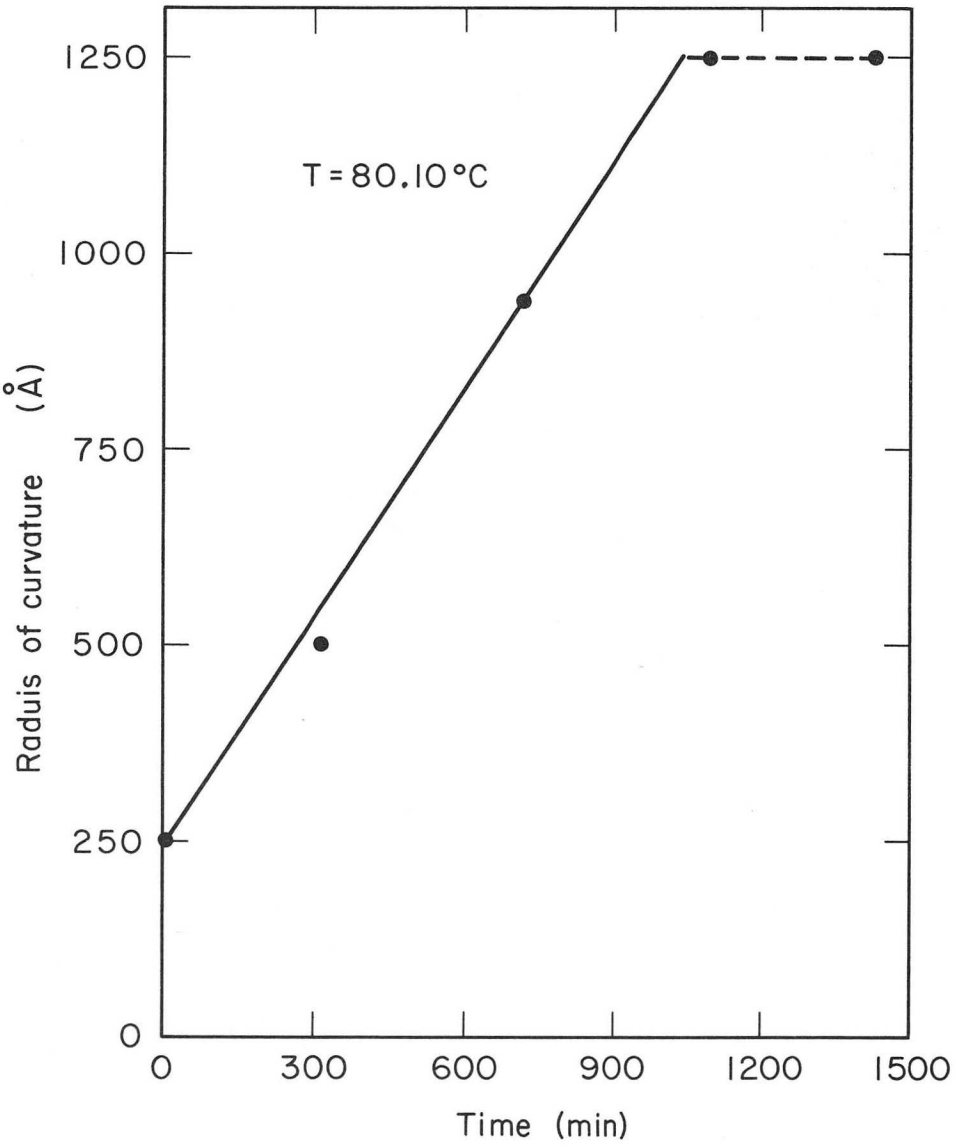

Fig. 9

MUB-11060

Fig. 9

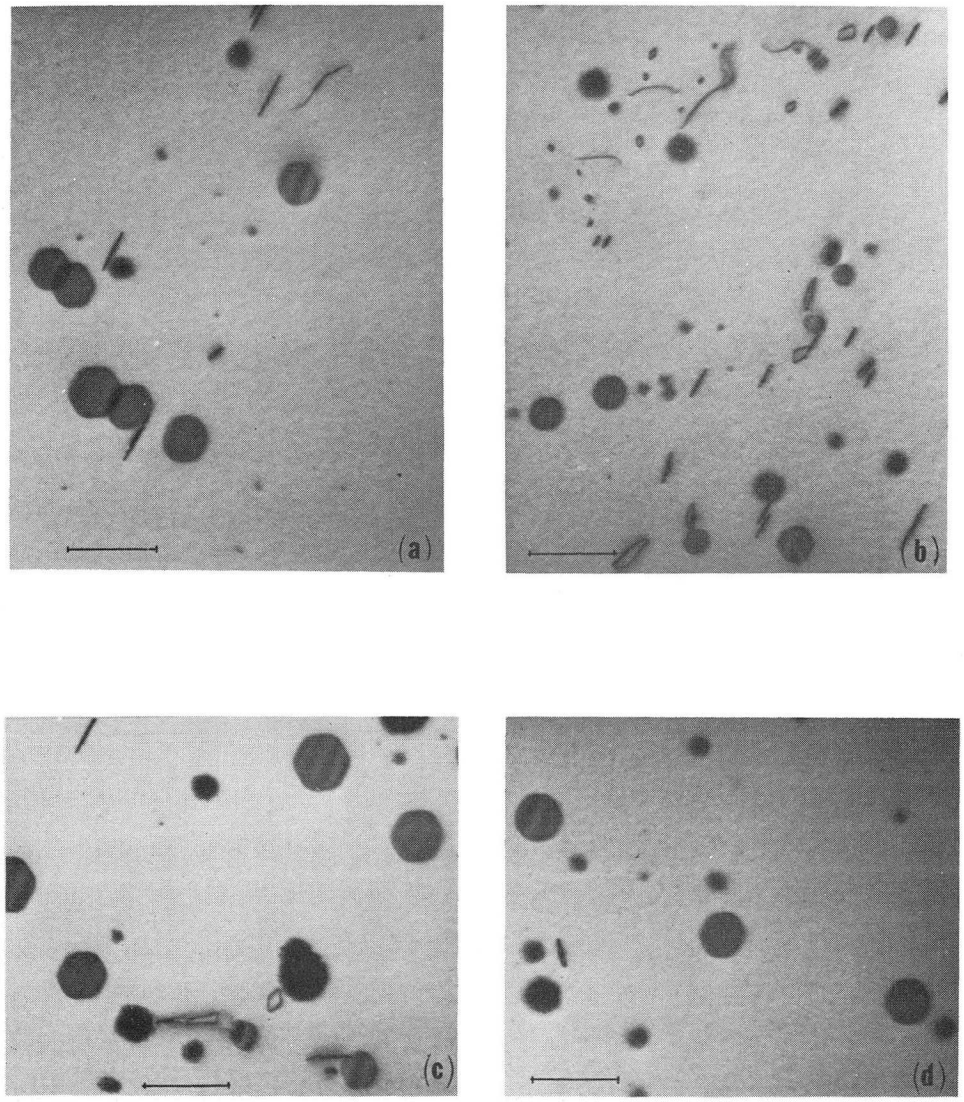

ZN-5876

Fig. 10abcd

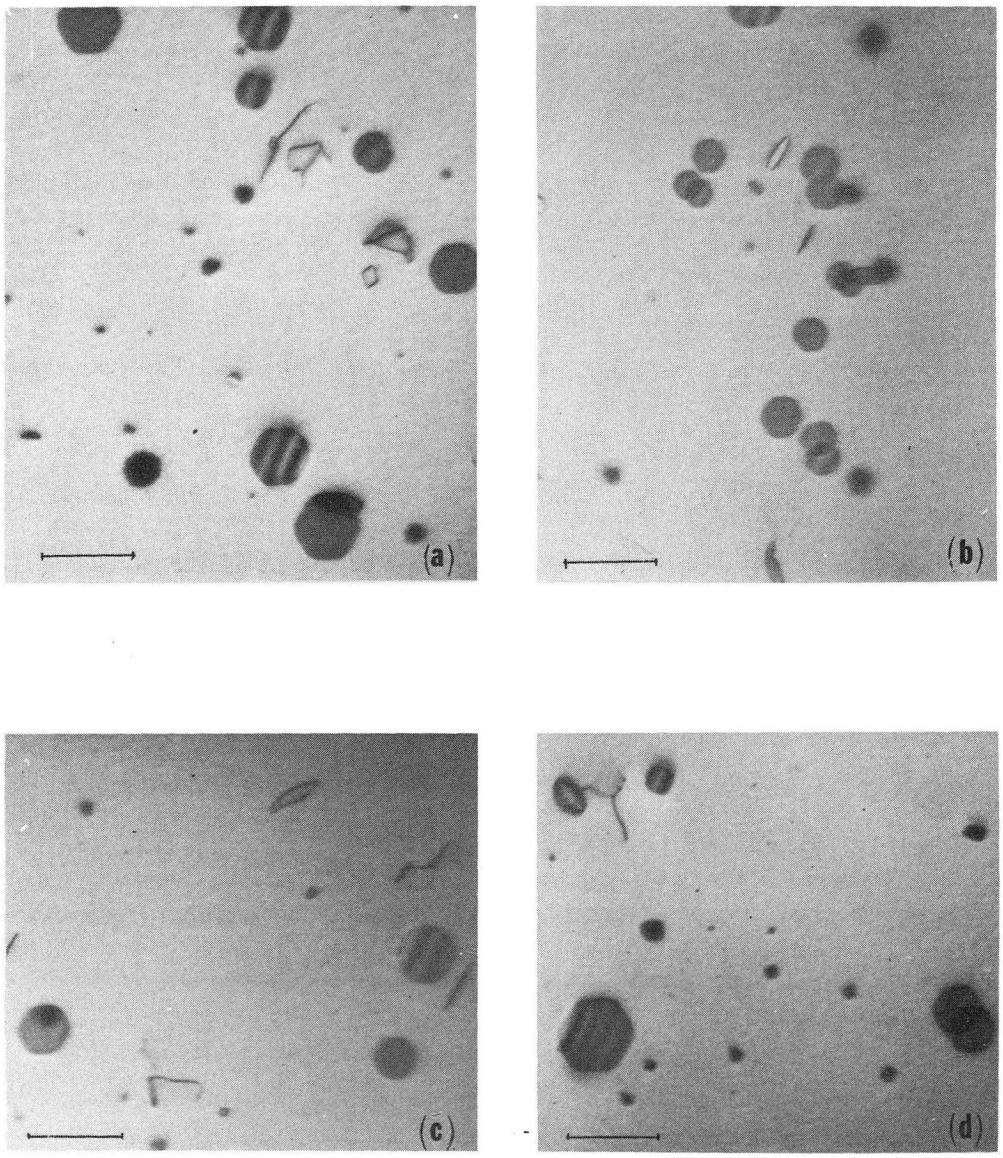

ZN-5880

Fig. 11abcd

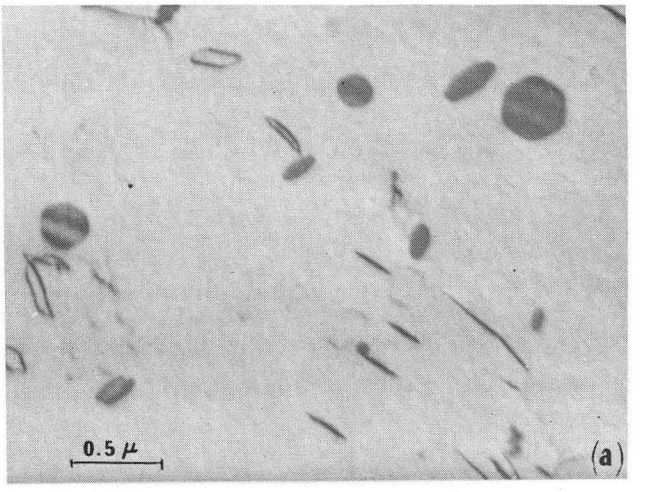

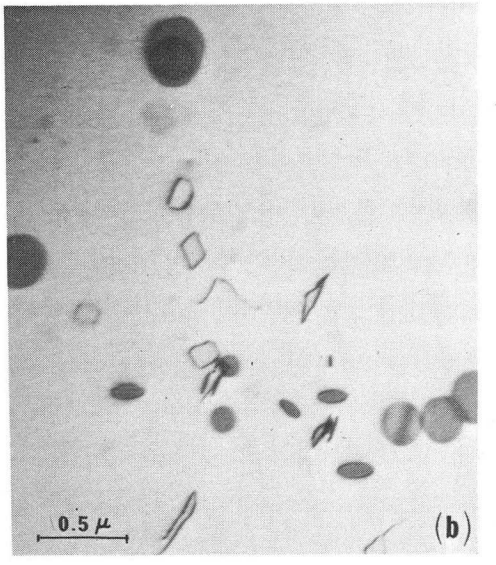

ZN-5879

Fig. 12ab

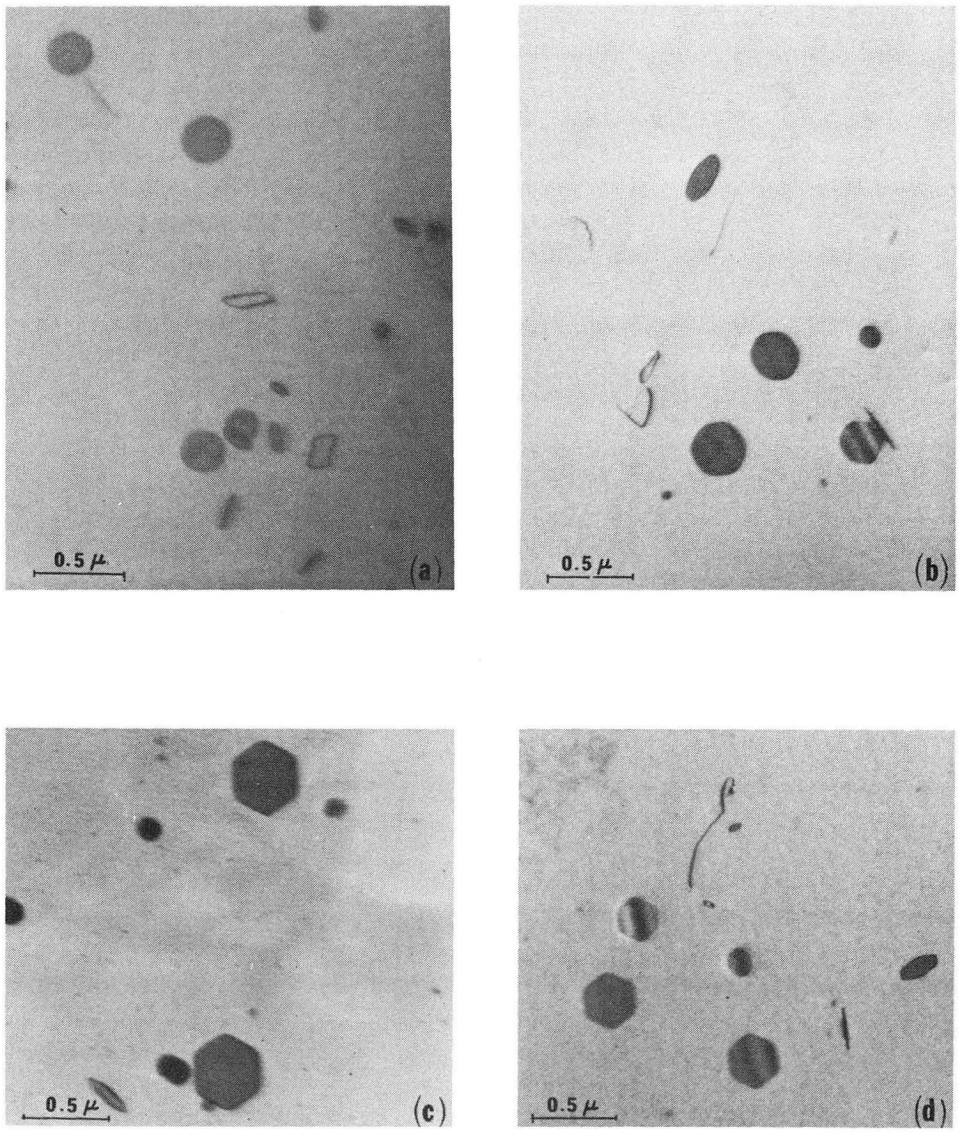

ZN-5874

Fig. 13abcd

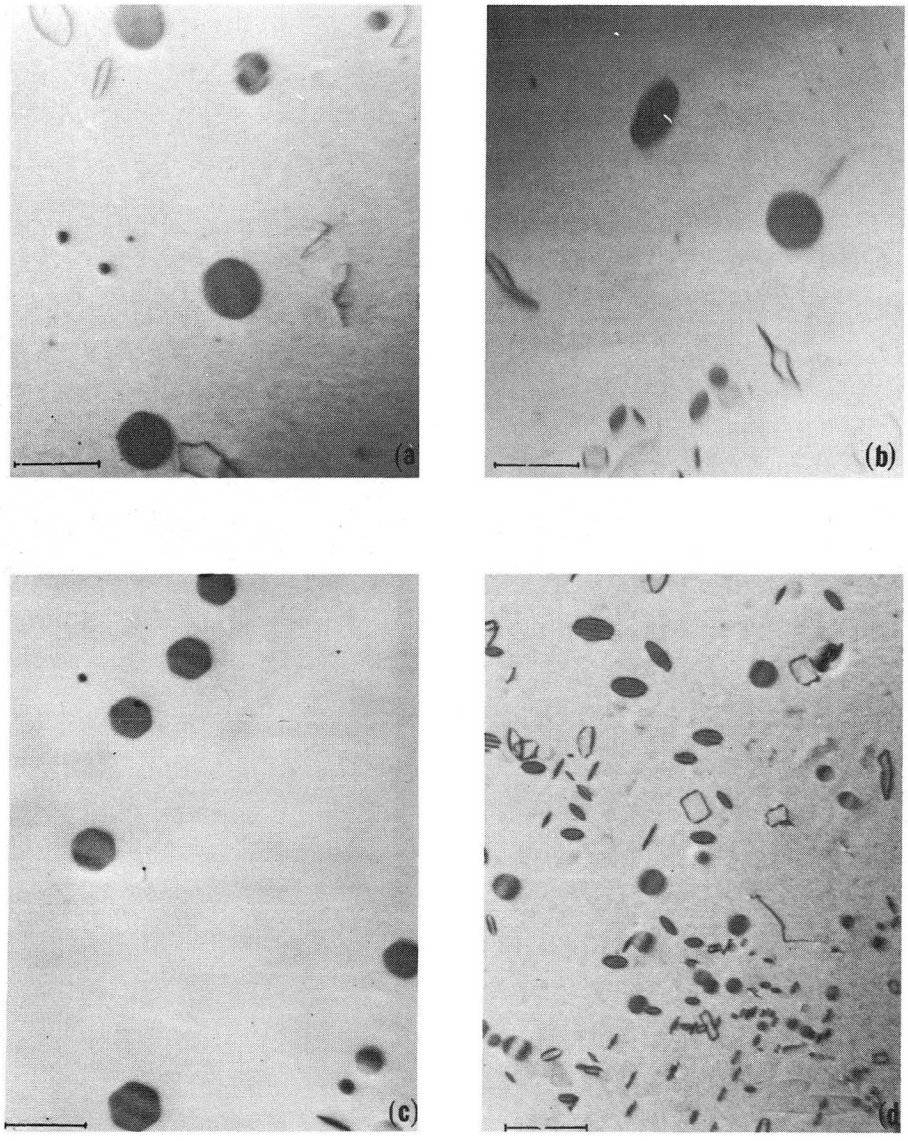

ZN-5883

Fig. 14abcd

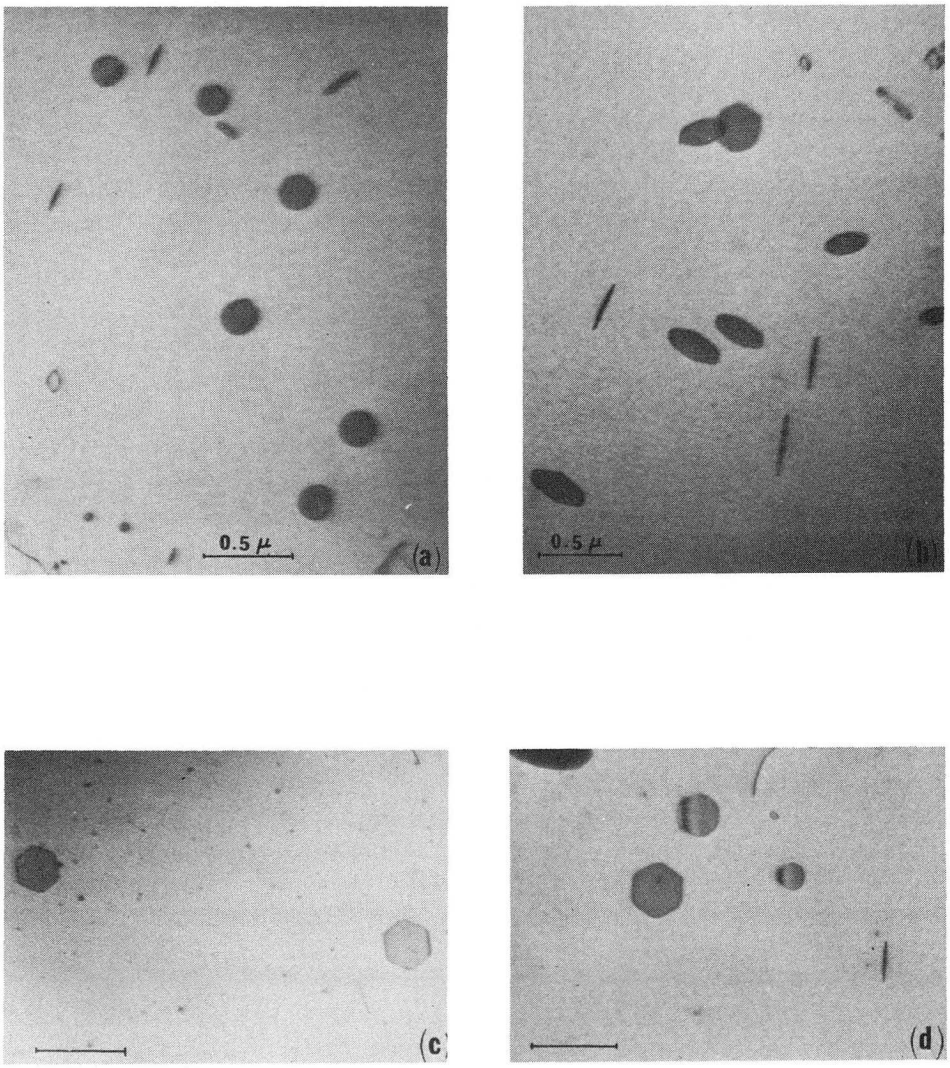

ZN-5882

Fig. 15abcd

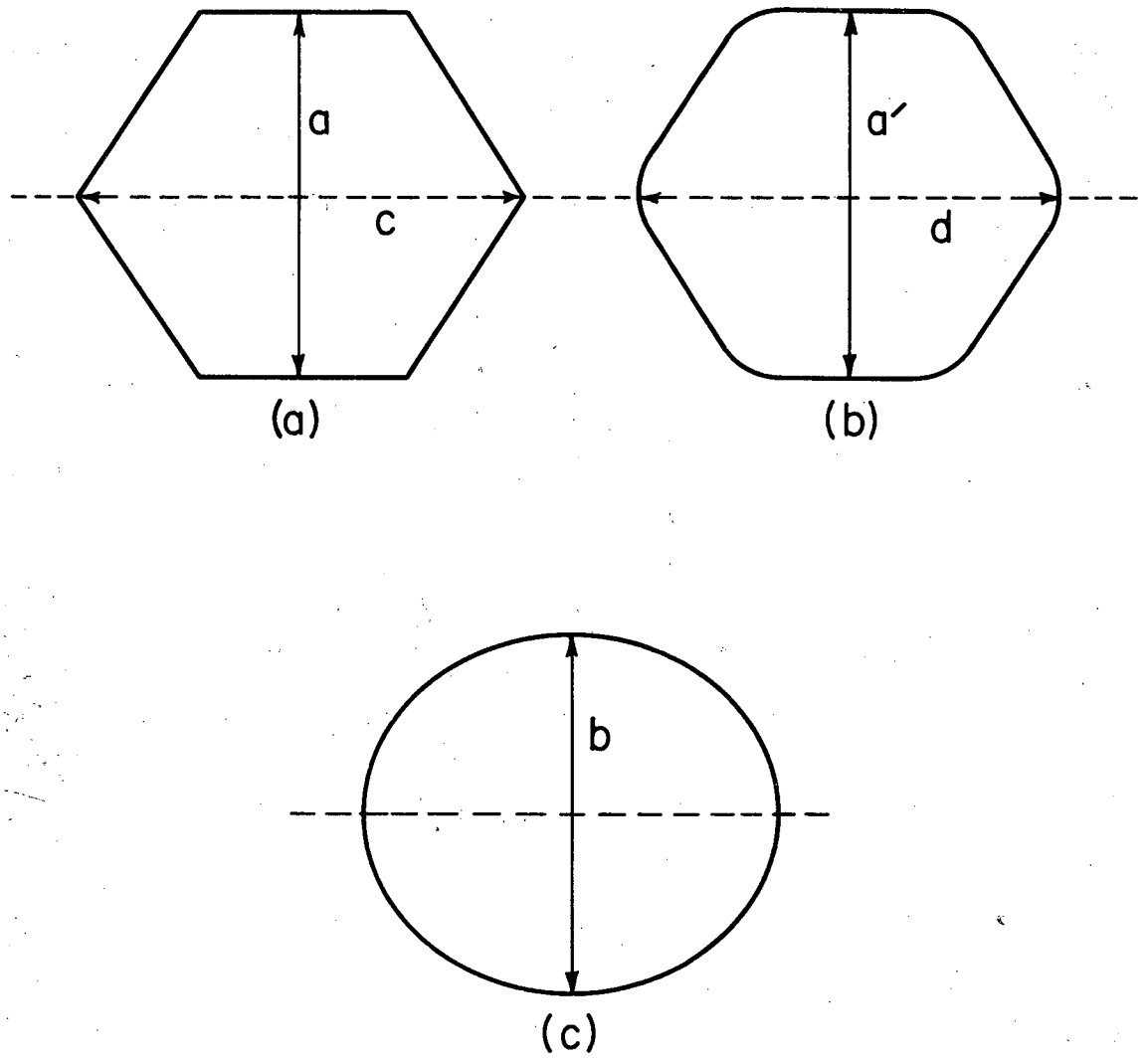

Fig. 16

MUB-11061

Fig. 16

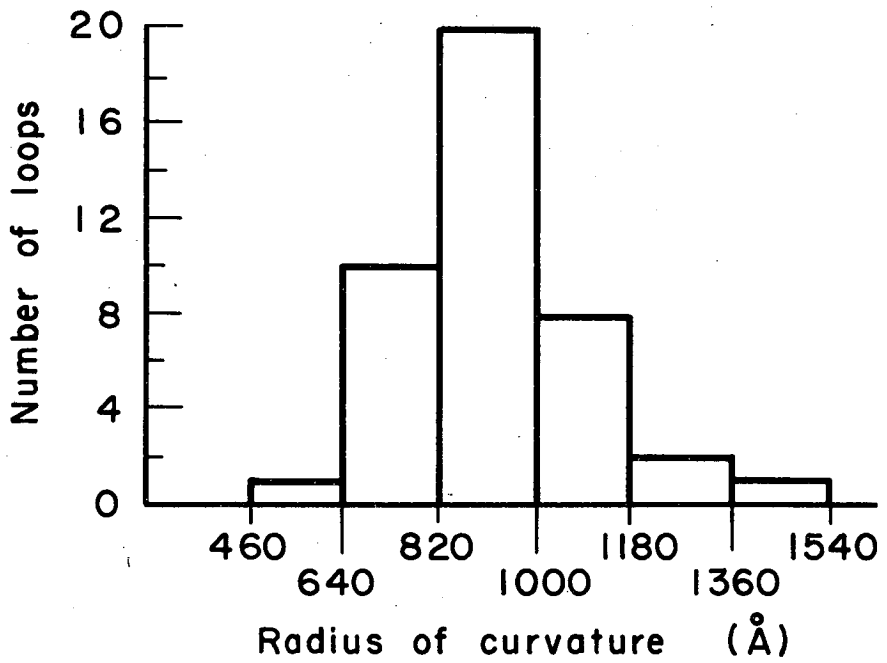

Fig. 17

MUB-11058

Fig. 17

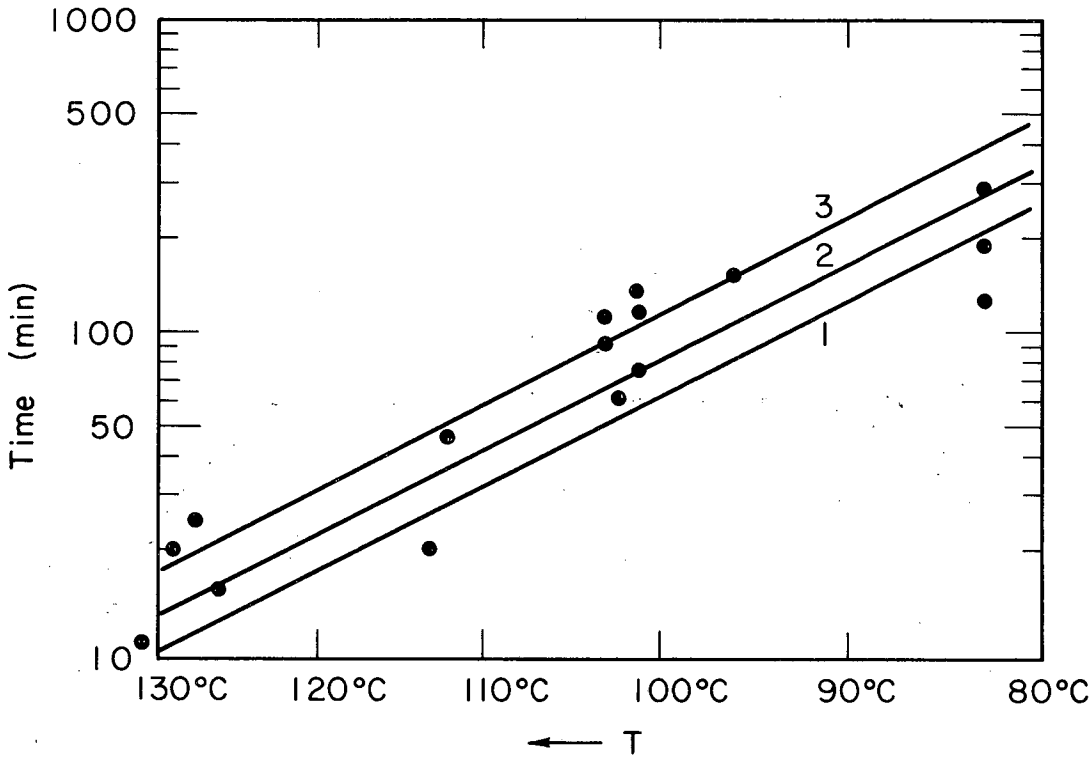

Fig. 18

MUB-11059

Fig. 18

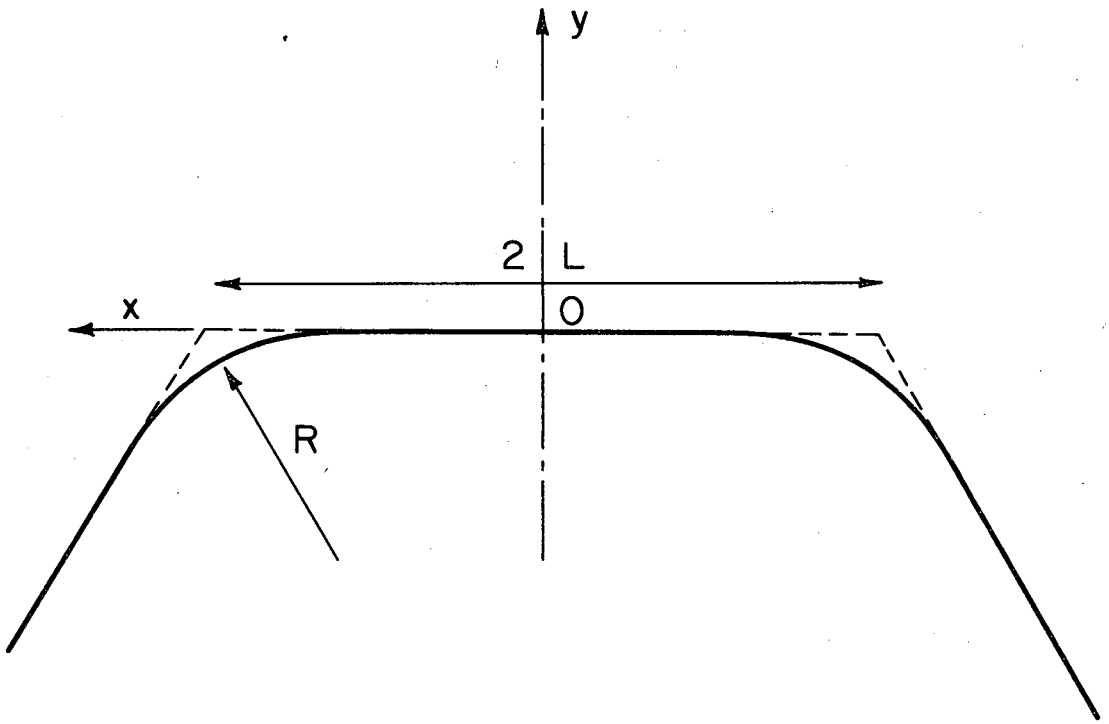

MUB-12453

Fig. 19

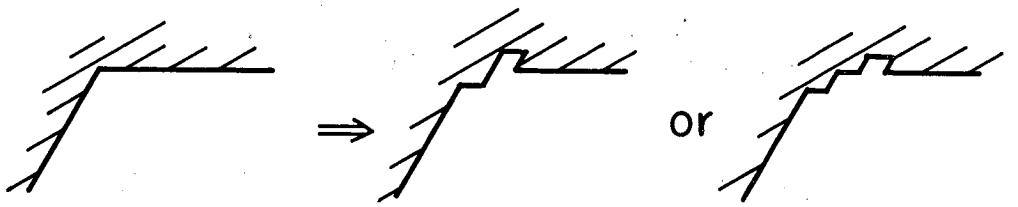

(a)

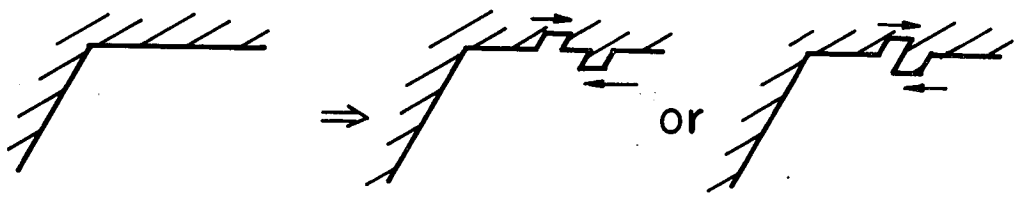

(b)

(c)

MUB-11525

Fig. 20abc

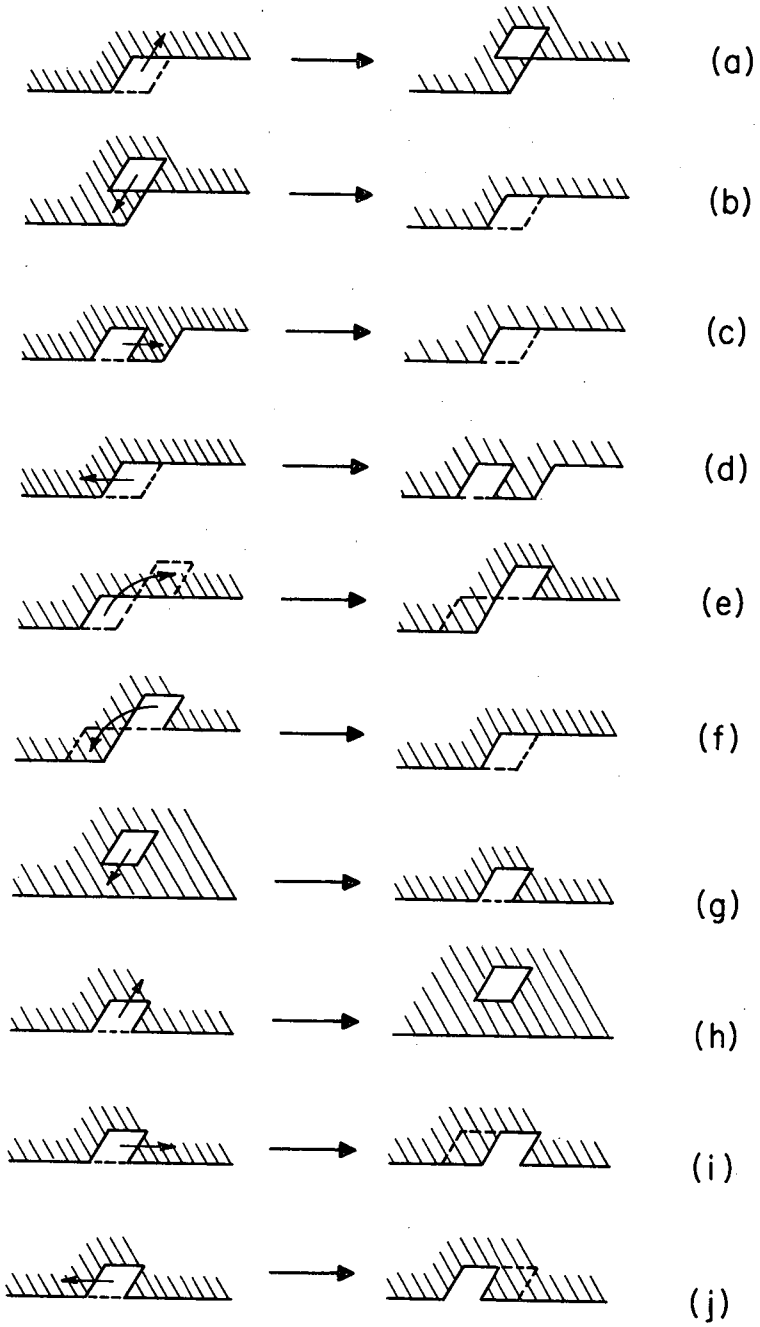

Fig. 21

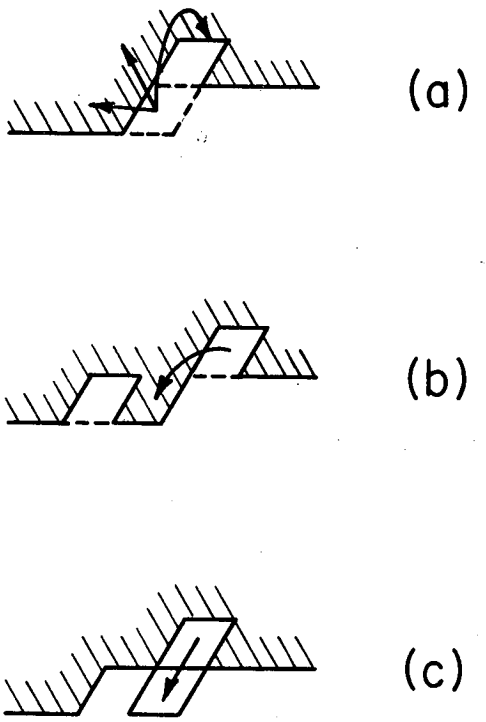

MUB 12454

Fig. 22abc

This report was prepared as an account of Government sponsored work. Neither the United States, nor the Commission, nor any person acting on behalf of the Commission:

A. Makes any warranty or representation, expressed or implied, with respect to the accuracy, completeness, or usefulness of the information contained in this report, or that the use of any information, apparatus, method, or process disclosed in this report may not infringe privately owned rights; or

B. Assumes any liabilities with respect to the use of, or for damages resulting from the use of any information, apparatus, method, or process disclosed in this report.

As used in the above, "person acting on behalf of the Commission" includes any employee or contractor of the Commission, or employee of such contractor, to the extent that such employee or contractor of the Commission, or employee of such contractor prepares, disseminates, or provides access to, any information pursuant to his employment or contract with the Commission, or his employment with such contractor.